

# Traffic Signal Control with Communicative Deep Reinforcement Learning Agents: a Case Study

Paolo Fazzini<sup>1</sup>, Isaac Wheeler<sup>2</sup>, and Francesco Petracchini<sup>1</sup>

<sup>1</sup>Institute of Atmospheric Pollution Research, CNR, Rome,  
Italy

<sup>2</sup>Department of Chemical Engineering Brigham Young  
University Provo UT 84602 United States

February 2021

Contact Author: Paolo Fazzini Email: paolo.fazzini@iia.cnr.it  
Address: c/o CNR-IIA, Via Salaria Km 29,300 - 00015 Monterotondo(Rome),  
Italy

## Abstract

In this work we analyze Multi-Agent Advantage Actor-Critic (MA2C) a recently proposed multi-agent reinforcement learning algorithm that can be applied to adaptive traffic signal control (ATSC) problems. To evaluate its potential we compare MA2C with Independent Advantage Actor-Critic (IA2C) and other Reinforcement Learning or heuristic based algorithms. Specifically, we analyze MA2C theoretically with the framework provided by non-Markov decision processes, which allows a deeper insight of the algorithm, and we critically examine the effectiveness and the robustness of the method by testing it in two traffic areas located in Bologna (Italy) simulated in SUMO, a software modeling tool for ATSC problems. Our results indicate that MA2C, trained with pseudo-random vehicle flows, is a promising technique able to outperform the alternative methods.

***Keywords***— Adaptive Traffic Signal Control, Non-Markov Decision Process, Multi-Agent System, Reinforcement Learning, Vehicle Flow Optimization

## 1 Introduction

With the constantly increasing demand for transportation, especially in the goods-and-services market, creating an efficient control system for traffic logistics is of paramount importance. Such a system could reduce air pollution, noise, vehicle accidents, and cost of transportation. These observations naturally lead to the

issue of how to efficiently coordinate signalized intersections to reduce traffic congestion. In recent years, various attempts to manage traffic logistics have been proposed. These strategies were initially intuition-driven directives, such as the Greedy strategy, which simply states that longest local queues should be released first. However, more elaborated approaches exploiting knowledge of the complex dynamics between the vehicle flows are needed in order to manage the complicated challenges posed by real traffic networks. The increasing success of machine learning and data mining techniques suggests applying various artificial-intelligence based algorithms to the problem of managing traffic signal control.

In this work we evaluate an algorithm called Multi-Agent Actor-Critic (MA2C [1] [2]), in two areas of the city of Bologna (Italy), namely the Andrea Costa and the Pasubio areas, and compare its performance with Independent Actor-Critic (IA2C), Independent Q-Learning Deep Neural Network (IQL-DNN), Independent Q-Learning Linear Regression (IQL-LR)<sup>1</sup> ([1]), and with the Greedy algorithm which simply states that longer queues of vehicles should be released first. In our traffic networks, replicated in SUMO<sup>2</sup>, signalized intersections are considered as agents engaged in a stochastic game whose goal is to reduce traffic congestion. After discussing the theoretical foundations of the algorithms and their relation with conventional multi-agent deep reinforcement learning we analyze their efficacy and robustness.

---

<sup>1</sup>The latter two Q-learning based RL algorithms differ from each other for the way they fit the Q-function, whether they use Linear Regression or a Deep Neural Network

<sup>2</sup>SUMO [3] a micro-traffic simulator capable to simulate traffic dynamics

## 1.1 Related Work

Adaptive traffic signal control (ATSC) aims for reducing potential congestion in signalized road networks by adjusting the signal timing according to real-time traffic dynamics [1]. In the early eighties, ATSC gained popularity as a result of the success of SCOOT (Split Cycle and Offset Optimisation Technique) [4], developed in the UK and SCATS (Sydney Coordinated Adaptive Traffic) [5] developed in Australia.

Since then several techniques have been applied to optimization problems of this kind such as Fuzzy Logic [6], [7], swarm intelligence [8], Genetic Algorithms [9], and Reinforcement Learning (in a variety of instances such as q-learning, double q-learning, dueling networks, and Actor-Critic), which yield promising results when applied in a multi-agent context. In a nutshell, Reinforcement Learning is a machine learning method to design agents that learn to perform a task by interacting with an external environment and by receiving a reward signal indicating how well they are doing. Such a paradigm can be scaled to a multi-agent scenario: in the ATSC case, agents controlling multiple traffic lights are trained to minimize traffic congestion. By allowing the agents to observe the environment and to receive information from other agents, the system can achieve an optimum behavior in its entirety. However full observation and total information sharing becomes a limiting factor when the number of agents grows. The four Multi-Agent Reinforcement Learning methods evaluated in this work, namely MA2C ([1], [2]), IA2C, IQ-L-DNN and IQ-L-LR ([1]) differ in that respect. The agents operate on the basis of local observation in all cases. However, in the IA2C, IQ-L-DNN and IQ-L-LR cases the agents learn from a reward measuring the global traffic and are

not allowed to communicate. In the MA2C case, instead, the agents learn from a reward function that measures the local traffic only and are allowed to communicate by observing the actions of nearby agents. Convergence constitutes a challenge for distributed approaches of this kind. This is due to the fact that the modification of the behavior of an agent, during the learning phase, can create the need for a consequent modification of the behavior of the other agents, which, in turn, might trigger further changes in the original agent’s action. These effects might yield unsteady dynamics in which the agents’ behaviour keep changing continuously, in the attempt to adapt to variations caused by other agents, without converging to a steady state.

## 1.2 Paper Plan

The remainder of this paper is organized as follows. Section 2.1 describes intuitively how a traffic network can be seen as an instance of MARL and section 2.2 formalizes such concepts from a single agent standpoint. Section 2.2.1 extends this formalism to the multi-agent case. In Section 2.3, we present the theoretical foundations of MA2C and IA2C framing them in a non-Markov scheme: first we review the actor-critic machinery from a single (2.4.1) and multiple (2.5) viewpoint and then present the IA2C (2.5.1) and MA2C (2.5.2) formalism. The implementation of the described algorithms is shown in section 2.6 and 2.6.1. In section 3, we present our experiments and in section 4 the learning graphs are analyzed. Section 5 summarizes our results in terms of general vehicle flow. Finally, we conclude the study with a discussion of the presented topics and future directions in Section 6 and 7.

## 2 Material and Methods

Figure 1 shows a typical setting for our experiments: a traffic network including multiple signalized intersections controlled by corresponding agents. Every intersection contains one or more crossroads, each including a number of lanes.

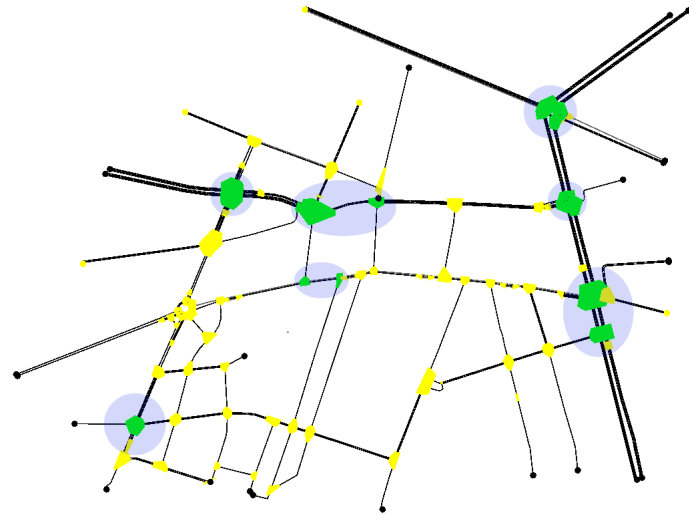


Figure 1: Traffic network: the shaded round spots (light blue) reference the signalized intersections (agents); their respective crossroads, contained in the round spots, are highlighted in dark (green) colour; the crossroads not controlled by traffic lights are highlighted in light (yellow) color.

### 2.1 System Overview

In all the methods considered (IQL-DNN, IQL-LR, IA2C and MA2C), each agent observes the nearby vehicle flow and outputs an action vector determining the traffic light switching. In MA2C, however, agents also observe the behavior of their neighbors, i.e. the strategy of agents located in nearby intersections. Agents trained with MA2C, therefore, receive more information than the agents trained

with the other methods. In all cases, however, they operate on the basis of partial information (they are not able to observe the entire state of the environment).

Another peculiarity of MA2C lies in the way the reward is calculated. In IQL-DNN, IQL-LR and IA2C, rewards encode the overall traffic; in MA2C, instead, rewards encode local traffic only. The two methods have potentially positive and negative sides. Indeed, a measure of the overall traffic forces the agents to cooperate but let the learning process of each agent to be driven by a measure that is only weakly correlated with the actions produced by each agent. Adopting a measure of the local traffic, instead, does not guarantee cooperation but allows rewarding each agent based on a measure that is more centered to its actions. Moreover, such a measure can promote competition between distant agents yielding convergence towards better strategies in each group of agents. These differences among IQL-DNN, IQL-LR, IA2C and MA2C also impact the stability of the learning dynamics.

## 2.2 System Formalization

From an agent's standpoint, the problem of coordinating signalized intersections can be formalized as it follows: every *agent* (i.e. every signalized intersection) aims to minimize the amount of queuing vehicles (*reward*<sup>3</sup>) by observing their motion in its neighborhood (i.e. by observing its neighborhood *state*) and ultimately learns how to balance its *actions* (by controlling traffic lights switching) with the other agents. However, while the IA2C agent type observes only its neighborhood and, seeking its best possible strategy (*policy*<sup>4</sup>), encodes in its reward computation the

---

<sup>3</sup>to comply the literature on the subject, in this work we refer this quantity as *reward* even though the length of a vehicle queue is provided (and perceived) as a penalty

<sup>4</sup>*strategy* and *policy* refer similar entities although the former is more used in game theory, while the latter is more popular in reinforcement learning; in this work these two

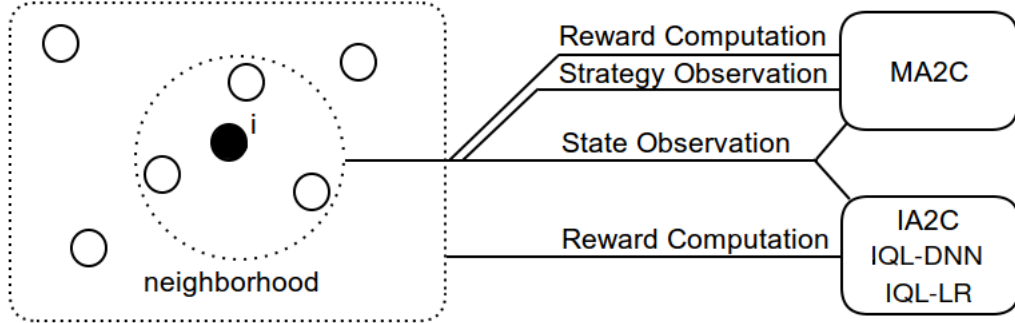


Figure 2: Agent  $i$  Reward and Observation in MA2C, IA2C, IQN-DNN and IQN-LR. The dotted rounded rectangle represents a traffic network (*environment*), the plain circle is Agent  $i$  while the empty circles refer the other agents; the dotted circle represents Agent  $i$ 's neighborhood.

vehicle queuing at traffic lights in the whole traffic network (*environment*), the MA2C agent type embeds in its state also the observation of its neighbors' policy (*fingerprints*), and restricts the environment reward to its neighbourhood (Figure 2).

### 2.2.1 Multi-Agent Formalization

Formally, a network of agents can be symbolized by a graph  $G(\mathcal{V}, \mathcal{E})$ , where  $\mathcal{V}$  (vertices) is the set of the agents and  $\mathcal{E}$  (edges) is the set of their connections, agent  $i$  and agent  $j$  are neighbors if the number of edges connecting them is less or equal some prefixed threshold. In the adopted formalism the neighborhood of agent  $i$  is denoted as  $\mathcal{N}_i$  and its local region is  $\mathcal{V}_i = \mathcal{N}_i \cup i$ . The distance between any two agents is denoted as  $d(i, j)$  with  $d(i, i) = 0$  and  $d(i, j) = 1$  for any  $j \in \mathcal{N}_i$ .

The following list summarizes how the above introduced entities are defined in  
 terms are used interchangeably

this setting:

- Agent: Signalized Intersection
- Environment: Traffic Network
- Reward:

The one-step reward for agent  $i$  at time  $t$  cumulates the queues (number of vehicles with speed less than 0.1 m/s) at the lanes converging to a certain signalized intersection in the interval  $[t, t + \Delta_t]$ :

$$r_{t,i} = \sum_{ji \in \mathcal{E}, l \in L_{ji}} queue_{t+\Delta t}[l]$$

where  $L_i$  is the set of lanes converging at a signalized intersection (agent)  $i$ . The one-step reward is accrued over multiple steps to form the Reward perceived by agent  $i$  (this step is different in MA2C, with respect to the other algorithms, as detailed in the following sections).

- State (IA2C, IQL-DNN and IQL-LR):

The state of the IA2C, IQL-DNN and IQL-LR agents at time  $t$  ( $s_t$ ) is computed by:

$$s_{t,i} = \{wave_t[l_{ji}]\}_{l_{ji} \in L_i}$$

where  $wave_t$  [veh] measures the total number of approaching vehicles in the set of incoming lanes ( $L_i$ ) at time  $t$ , within 50m from a signalized intersection (agent  $i$ ).

- Action:  $u_{t,i}$  is the action of agent  $i$  at time  $t$  (traffic light setting)

- Policy:

agent  $i$ 's policy at time  $t$  ( $\pi_{t,i}$ ) is a the probability distribution over its available actions

- Fingerprints:

policy vector of agent  $i$ 's neighbor agents ( $\pi_{t,-i}$ )

- State (MA2C):

$$s_{t,i} = [\alpha \cdot s_{t,i}^{IA2C}, \pi_{t,-i}]$$

where  $\alpha$  is a multiplication factor limiting the neighbor agents observation ( $\alpha < 1$ ).

In this document, the states of all the considered agents will simply be referred to as  $s_t$  when the context prevents confusion.

### 2.3 Background

In [1] all the algorithms have been developed assuming a Markov environment. However, as MA2C and IA2C rely on the history of past state observations stored in a LSTM network, we build their formalism in the framework of recurrent policy gradients [10]. In this view the goal is to learn limited-memory stochastic policies  $\pi(u_t | h_t)$ , i.e. policies that map sufficient statistics of a sequence of states  $h_t$  to probability distributions on actions. For IQL-DNN and IQL-LR we refer to [1] for a fully detailed description of the algorithms.

## 2.4 Markov Decision Process

Reinforcement learning (RL) can be used to find optimal solutions for many problems. A Markov Decision Process (MDP) constitutes an adequate framework for Markovian approaches such as IQL-DNN and IQL-LR. An MDP can then be defined as a tuple  $(\mathcal{S}, \mathcal{U}, P, R, \gamma)$  with its contents defined as follows:

- $\mathcal{S}$  is a set of states, where  $s_t \in \mathcal{S}$  denotes the agent's state at time  $t$ .
- $\mathcal{U}$  is a set of available actions, where  $u_t \in \mathcal{U}$  denotes the action the agent performs at time  $t$ .
- $p : \mathcal{S} \times \mathcal{U} \times \mathcal{S} \rightarrow [0, 1]$  is a transition function and denotes the probability of ending up in state  $s_{t+1}$  when performing action  $u_t$  in state  $s_t$ .
- $r : \mathcal{S} \times \mathcal{U} \times \mathcal{S} \rightarrow \mathbb{R}$  is a reward function where  $r_{t+1}$  is the reward when the agent transitions from state  $s_t$  to state  $s_{t+1}$  after performing action  $u_t$ .
- $\gamma \in [0, 1]$  is a discount factor.

The transition function  $p$  is often referred as the model of the system as it captures its dynamics. However, in the implementation of IQL-DNN and IQL-LR [1], every action  $u_t$  yields a state change  $s_t \rightarrow s_{t+1}$  with probability equal one, consequently zeroing the probability of any other transition. In general  $\mathcal{U}$  might depend on  $s_t$  but we restrict our reasoning to the case where it doesn't change.

### 2.4.1 Single Agent Recurrent Policy Gradients

For IA2C and MA2C, which are equipped with a memory as discussed in the next sections, we no longer rely on the MDP described in 2.4. In this case the

environment still produces a state  $s_t$  at every time step but state transitions are governed by a probability function  $p(s_{t+1} | u_{1:t}, s_{1:t})$  (also referred to as the *model*) unknown to the agent and dependent upon all its previous actions  $u_{1:t}$  and all the previous states  $s_{1:t}$  of the system.

In this, more general, setting, the agent has a memory of its experience consisting of finite episodes. Such episodes are generated by the agent's behaviour in the environment: the agent performs action  $u_t$  at every time step  $t$ , after observing  $s_t$  and receives a reward  $r_t$  whose expectation depends solely on  $u_t$  and  $s_t$ . We define the observed history  $H_t$  as the sequence of states and actions up to moment  $t$  since the beginning of the episode:  $H_t = [s_0, u_0, \dots, s_{t-1}, u_{t-1}, s_t]$ .

With an optimal or near-optimal policy for a non-Markov Decision Process (non-Markov DP) the action  $u_t$  is taken depending on the preceding history. Let  $R(H_t)$  be a measure of the total reward accrued during a sequence of states, and let  $p(H_t | \theta)$  be the probability of a state sequence given policy-defining weights  $\theta$ , then the quantity to minimize is  $\tilde{\mathcal{L}}(\theta) = \int p(H_t | \theta)R(H_t)dH_t$ . This, in essence, indicates the expected reward over all possible (selectively remembered) sequences, weighted by their probabilities. Using gradient descent to update parameters  $\theta$  we can write:

$$\nabla_{\theta}\tilde{\mathcal{L}}(\theta) = \nabla_{\theta}\mathbb{E}_{H_t}[R(H_t)] = \int \nabla_{\theta}p(H_t)R(H_t)dH_t = \int p(H_t)\nabla_{\theta}\log p(H_t)R(H_t)dH_t$$

using the likelihood-ratio "trick" [11] and the fact that  $\nabla_{\theta}R(H_t) = 0$  as the accrued reward  $R(H_t)$  does not depend on  $\theta$ . Accordingly, the loss can be rewritten as:

$$\tilde{\mathcal{L}}(\theta) = \mathbb{E}_{H_t} [\log p(H_t) R(H_t)]$$

where  $p(H_t)$  is the only term depending on  $\theta$ .

In the above computations, we considered the whole state-action sequence  $H_t$ . However, the whole sequence is not needed and the agent needs to learn only sufficient statistics (*history* henceforth)  $h_t = S(H_t)$  of the events which we call the limited memory of the agents' past. Thus, a stochastic policy  $\pi$  and an history  $h_t$  can be redefined by the position  $\pi(u | h_t; \theta) = \pi(u | S(H_t); \theta)$ <sup>5</sup>, and implemented as an RNN of type LSTM with weights  $\theta$ . This produces a probability distribution  $\pi(u | h_t)$ , from which actions are drawn. Accordingly,  $p(H_t)$  can be further subdivided:

$$p(H_T) = p(s_0) \prod_{t=1}^T p(s_t | u_{t-1}, s_{0:t-1}) \pi(u_{t-1} | h_{t-1})$$

as in the Markov policy gradient case, all the  $p$  terms will be split in a sum of logarithms and can be removed, since they don't depend on  $\theta$ . The final loss is:

$$\tilde{\mathcal{L}}(\theta) = \mathbb{E}_{H_t} [\log \pi(h_t) R(H_t)]$$

Performing Monte Carlo sampling for the whole episode length:

$$\tilde{\mathcal{L}}(\theta) \approx \sum_{i=0}^{N_{sa}-1} \sum_{t=0}^{N_{st}-1} \log \pi(u_{t,i} | h_{t,i}) \hat{R}_{t,i} \quad (1)$$

Where  $N_{sa}$  is the number of sampled episodes and  $N_{st}$  is the number of time

---

<sup>5</sup>To lighten our notation, in some cases the dependence from  $\theta$  will be omitted if clear from the context

steps in an episode.

Introducing batch learning and iterating over sampled episodes, the training procedure aims to minimize the following loss.

$$\mathcal{L}(\theta) = \sum_{t=0}^{t_B-1} \log \pi(u_t|h_t) \hat{R}_t \quad (2)$$

Where the episode index has been omitted.

In equation (2),  $t_B$  is the number of time steps in the batch;  $\hat{R}_t = \sum_{\tau=t}^{t_B-1} \gamma^{\tau-t} r_\tau$ , where the usual  $\gamma$  discount factor has been introduced [12], is the aggregated reward over the batch;  $r_\tau$  is sampled from  $\mathbb{E}[r_\tau^\pi]$ .

#### 2.4.2 Single Agent Recurrent Advantage Actor Critic

Following the formulation in section 2.4.1, we derive the loss functions for Recurrent Advantage Actor-Critic (A2C) for a non-Markov DP. the Actor's loss is:

$$\mathcal{L}(\theta) = \sum_{t=0}^{t_B-1} \log \pi_\theta(u_t|h_t^\pi) A_t \quad (3)$$

while the Critic's loss is:

$$\mathcal{L}(\psi) = \frac{1}{2} \sum_{t=0}^{t_B-1} (R_t - V_\psi(h_t^V))^2 \quad (4)$$

where:

- $h_t^\pi$  and  $h_t^V$  are the histories of past events registered by the two LSTM networks used to compute the regressors  $\pi_\theta$  and  $V_\psi$
- $R_t = \hat{R}_t + \gamma^{t_B-t} V_\psi(h_{t_B}^V)$  is the  $n$ -step return [12],  $n = t_B - t$ ; the regressor

for state value at  $t_B$  (corresponding temporally to the first time step of the next batch) is evaluated using the current parameters  $\psi^-$

- $A_t = R_t - V_{\psi^-}(h_t^V)$  is the sampled advantage for actions  $\{u_t, \dots, u_{t_B-1}\}$

in the above definitions,  $\psi^-$  is the set of the Critic's parameters computed at the last learning step (current Critic's parameters); correspondingly, in the next sections with  $\theta^-$  will be indicated the set of the Actor's parameters computed at the last learning step (current Actor's parameters)<sup>6</sup>. Notably, the inner states of the Critic's LSTM are not updated when computing  $V_{\psi^-}(h_{t_B}^V)$  as  $t_B$  corresponds to the first time step of the next batch. This prevents the state sequence (history) from being compromised when the state value is computed while processing the next batch.

## 2.5 Multi-Agent Policy-Gradient Systems

### 2.5.1 Independent Advantage Actor-Critic (IA2C)

In IA2C, each agent  $i$  learns its own policy  $\pi_{\theta_i}$  and value function  $V_{\psi_i}$  collecting experiences from its own DP. Observation of agent  $i$  is restricted to  $\mathcal{V}_i$ , i. e.  
 $s_{t,\mathcal{V}_i} := \{s_{t,j}\}_{j \in \mathcal{V}_i}$ .

The loss functions for Actor and Critic are:

$$\mathcal{L}(\theta_i) = \sum_{t=0}^{t_B-1} \log \pi_{\theta_i}(u_{t,i} | h_{t,\mathcal{V}_i}^\pi) A_{t,i} + \beta \sum_{u_i \in \mathcal{A}_i} \pi_{\theta_i} \log \pi_{\theta_i}(u_i | h_{t,\mathcal{V}_i}^\pi) \quad (5)$$

---

<sup>6</sup>In [1]  $\psi^-$  and  $\theta^-$  are referred as the *frozen* state-value and policy in order to include in the development an eventual frozen set of parameters staying constant during multiple learning steps. We prefer to avoid this terminology as in the implementation reported here the parameters get updated after each learning step

$$\mathcal{L}(\psi_i) = \frac{1}{2} \sum_{t=0}^{t_B-1} (R_{t,i} - V_{\psi_i}(h_{t,\mathcal{V}_i}^V))^2 \quad (6)$$

where:

- $A_{t,i} = R_{t,i} - V_{\psi_i^-}(h_{t,\mathcal{V}_i}^V)$
- $R_{t,i} = \hat{R}_t + \gamma^{t_B-t} V_{\psi_i^-}(h_{t_B,\mathcal{V}_i}^V)$
- $\hat{R}_t = \sum_{\tau=t}^{t_B-1} \gamma^{\tau-t} \hat{r}_\tau$
- $\hat{r}_t = \frac{1}{|\mathcal{V}|} \sum_{i \in \mathcal{V}} r_{t,i}$
- $h_{t,\mathcal{V}_i}^\pi = S^\pi(H_{t,\mathcal{V}_i})$
- $h_{t,\mathcal{V}_i}^V = S^V(H_{t,\mathcal{V}_i})$
- $H_{t,\mathcal{V}_i} = [\{s_{0,j}\}, u_0, \dots, \{s_{t-1,j}\}, u_{t-1}, \{s_{t,j}\}]$  with  $j \in \mathcal{V}_i$

In the above,  $\theta_i$  and  $\psi_i$  are the network Actor and Critic's parameters, and a ' $-$ ' superscript indicates their *current* values;  $-i$  as a parameter subscript refers all the agents apart agent  $i$ .

In the beginning of training all actions have similar probability so, to burst exploration, the entropy loss of policy  $\pi_{\theta_i}$  has been added in (5), weighted by the parameter  $\beta$ .

Restricting observation of agent  $i$  to  $\mathcal{V}_i$  affects both  $V_{\psi_i}$  and  $\pi_{\theta_i}$  via  $H_{t,\mathcal{V}_i}$ . On the one hand, this yields partial observability while on the other hand, being  $R_{t,i}$  dependent on the whole  $s_t$ , it allows  $\mathcal{V}_i$  and  $\pi_{\theta_i}$  to converge towards optimum values more specific of agent  $i$ . This is mostly evident for  $V_{\psi_i}$  as without restricting the agent's observation, all the agents will seek the same global optimum  $V^*$ , while every  $\pi_{\theta_i}$  has its own specification in terms of type and number of available actions.

### 2.5.2 Multi-Agent Advantage Actor-Critic (MA2C)

MA2C [1] improves the stability of the learning process by allowing some communication only among agents belonging to the same neighborhood: a spatial discount factor weakens the reward signals from agents other than agent  $i$  in the loss function and agents not in  $\mathcal{N}_i$  are not considered in the reward computation. Equations (5) and (6) become:

$$\begin{aligned} \mathcal{L}(\theta_i) = & \sum_{t=0}^{t_B-1} \log \pi_{\theta_i} \left( u_{t,i} | \tilde{h}_{t,\mathcal{V}_i}^\pi, \pi_{t-1,\mathcal{N}_i} \right) \tilde{A}_{t,i} \\ & + \beta \sum_{u_i \in \mathcal{A}_i} \pi_{\theta_i} \log \pi_{\theta_i} \left( u_i | \tilde{h}_{t,\mathcal{V}_i}^\pi, \pi_{t-1,\mathcal{N}_i} \right) \end{aligned} \quad (7)$$

$$\mathcal{L}(\psi_i) = \frac{1}{2} \sum_{t=0}^{t_B-1} \left( \tilde{R}_{t,i} - V_{\psi_i} \left( \tilde{h}_{t,\mathcal{V}_i}^V, \pi_{t-1,\mathcal{N}_i} \right) \right)^2 \quad (8)$$

In the above equations:

- $\tilde{A}_{t,i} = \tilde{R}_{t,i} - V_{\psi_i^-} \left( \tilde{h}_{t,\mathcal{V}_i}^V, \pi_{t-1,\mathcal{N}_i} \right)$
- $\tilde{R}_{t,i} = \hat{R}_{t,i} + \gamma^{t_B-t} V_{\psi_i^-} \left( \tilde{h}_{t_B,\mathcal{V}_i}^V, \pi_{t_B-1,\mathcal{N}_i} \right)$
- $\hat{R}_{t,i} = \sum_{\tau=t}^{t_B-1} \gamma^{\tau-t} \tilde{r}_{\tau,i}$
- $\tilde{r}_{t,i} = \frac{1}{|\mathcal{V}_i|} (r_{t,i} + \sum_{j \in \mathcal{V}_i, j \neq i} \alpha r_{t,j})$
- $\tilde{h}_{t,\mathcal{V}_i}^\pi = \{h_{t,i}^\pi\} \cup \alpha \{h_{t,j}^\pi, j \in \mathcal{N}_i\}$
- $\tilde{h}_{t,\mathcal{V}_i}^V = \{h_{t,i}^V\} \cup \alpha \{h_{t,j}^V, j \in \mathcal{N}_i\}$
- $\tilde{h}_{t,\mathcal{V}_i}^\pi = \tilde{S}^\pi \left( \tilde{H}_{t,\mathcal{V}_i} \right)$
- $\tilde{h}_{t,\mathcal{V}_i}^V = \tilde{S}^V \left( \tilde{H}_{t,\mathcal{V}_i} \right)$

- $\tilde{H}_{t,\mathcal{V}_i} = [\{s_{0,i}\} \cup \alpha\{s_{0,j}\}, u_0, \dots, \{s_{t-1,i}\} \cup \alpha\{s_{t-1,j}\}, u_{t-1}, \{s_{t,i}\} \cup \alpha\{s_{t,j}\}]$   
with  $j \in \mathcal{V}_i$

The spatial discount factor  $\alpha$  penalizes other agent's reward<sup>7</sup> and  $D_i$  is the limit of agent  $i$  neighborhood.

Equation (8) yields a more stable learning process since (a) fingerprints  $\pi_{t-1,\mathcal{N}_i}$  are input to  $V_{\psi_i}$  to bring in account  $\pi_{\theta_{-i}}$ , and (b) spatially discounted return  $\tilde{R}_{t,i}$  is more correlated to local region observations  $(\tilde{s}_{t,\mathcal{V}_i}, \pi_{t-1}, \mathcal{N}_i)$ . By inspection of equations (5), (6), (7), (8), the peculiarities of MA2C with respect of IA2C can be therefore summarized in: 1) MA2C uses fingerprints, 2) MA2C uses a spatial discount factor, 3) the overall reward ( $\hat{R}_{t,i}$  in MA2C) is computed on  $\mathcal{V}_i$  instead of the whole set of agents  $\mathcal{V}$ .

## 2.6 System Architecture

Figure 3 provides an overview of the system.

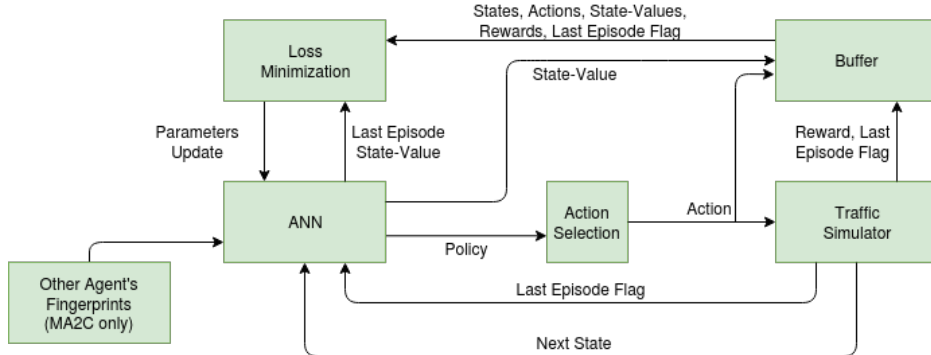


Figure 3: General Scheme: while seeking for an optimal Policy, Loss Minimization requires a repeated sequence of state-action-reward-next state steps.

<sup>7</sup>MA2C spatial discount factor highlights the competitive character of the mixed cooperative-competitive game among the agents with respect to IA2C

As stated in the previous sections, the goal is to minimize the vehicle queues measured at signalized intersections. To this end, the following steps are repeated: 1) an ANN takes as an input the perceived state of the environment eventually integrated (in the MA2C case only) with the policies of its neighbor agents (fingerprints) and provides a policy; 2) an action is sampled from the provided policy and passed to the Traffic Simulator, which, in turn, performs a simulation step, sends back to the ANN the new environment state and the Last Episode Flag (a flag indicating whether the episode is over) and store action, reward and Last Episode Flag in a buffer. These two steps are repeated until the buffer (in the following referred also as *batch*) is full. 3) the ANN uses the stored rewards to change its parameters in order to improve its policy.

### 2.6.1 ANN Detail

For IQL-DNN and IQL-LR we refer to the multi-perceptron ANN details in [1]. For MA2C and IA2C, states, actions, next states and rewards are collected in batches called experience buffers, one for each agent  $i$ :  $B_i = \{(s_t, u_t, s_{t+1}, r_t)\}_i$ . They are stored while the traffic simulator performs a sequence of actions. Each batch  $i$  reflects agent  $i$  experience trajectory. Figure 4 shows the IA2C and MA2C architectures. The network architecture reflects the A2C formalism [13], [14] therefore each graph represents two different networks, one for the Actor (Policy) and one for the Critic (State-Value). In the IA2C case, wave states are fed to a fully connected (FC) Layer with a variable number of inputs, depending by the number of lanes converging to the controlled signalized intersection. The output of the FC

layer (128 units) feeds the Long Short-Term Memory module (LSTM) equipped with 64 outputs and 64 inner states. The output of the LSTM module is linked to the network output that in the Actor’s case is a policy vector (with softmax activation function) and in the Critic’s case is a State-Value (with linear activation function). All the activation functions in the previous modules are Rectification Units (ReLU). The MA2C architecture differs from IA2C for the presence of the fingerprints unit (whose size depends by the number of available actions for the neighbor agents) which feeds the respective LSTM module through a separated FC layer. In Figure (4) the network biases are not depicted although present in each layer. For ANN training, an orthogonal initializer [43] and a gradient optimizer of type RMSprop have been used. To prevent gradient explosion, all normalized states are clipped to  $[0, 2]$  and each gradient is capped at 40. Rewards are clipped to  $[-2, 2]$ .

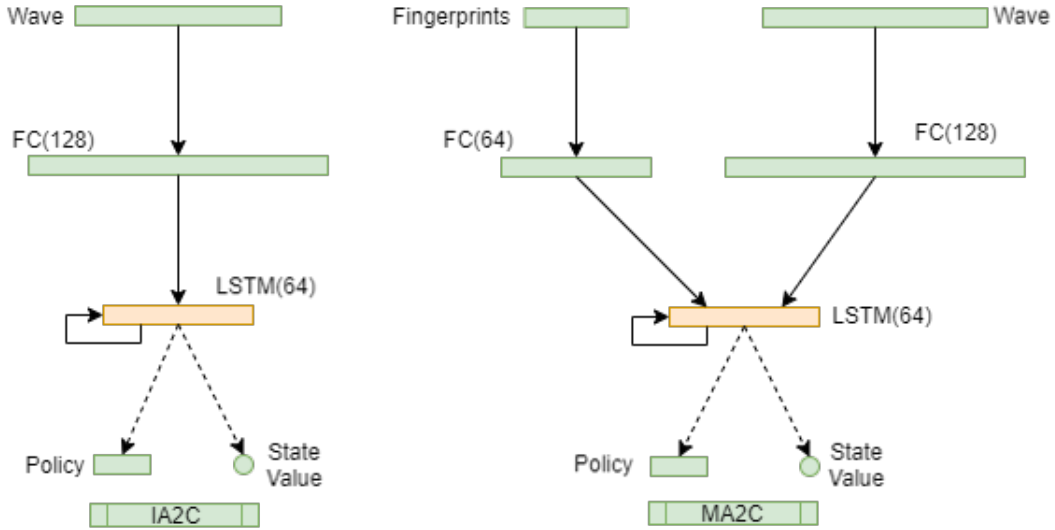


Figure 4: ANN Scheme of IA2C and MA2C

This architecture is used for each agent so  $2|\mathcal{V}|$  ANN's are instantiated. In IA2C (left), the first layer is formed by a variable number of input neurons that encode wave measures, i.e. the total number of approaching vehicles along each incoming lane, within 50m. The second layer is formed by 128 neurons. The third layer is formed by 64 LSTM units. The first layer is fully connected to the second layer. The third layer is fully connected to itself and to the fourth layer.

In the case of the MA2C method (Figure 4., right), the first layer is formed by a variable number of input neurons encoding wave measures and by a variable number of neurons encoding the action vectors of nearby agents. The second layer is formed by two groups of 128 and 64 neurons that receive connections from the two groups sensory neurons described above. The third layer is formed by 64 LSTM units. The first layer is fully connected to the second layer, the third layer is fully connected to itself and to the fourth layer.

The network architecture reflects the A2C formalism [13], [14] therefore each graph represents two different networks, one for the Actor (Policy) and one for the Critic (State-Value), their respective parameters being further referred as  $\theta$  and  $\psi$ . in the case of the Actor network the fourth layer is formed by  $N$  neurons update by using a softmax activation function. The  $N$  neurons encode the probabilities of choosing one of the  $N$  corresponding possible red-green-yellow transitions of the corresponding traffic light. In the case of the critic network, the fourth layer is formed by a single neuron that encodes the expected reward. The neurons of the second and third layer use the Rectification Units (ReLU) activation function. For ANN training, an orthogonal initializer [43] and a gradient optimizer of type RMSprop have been used. To prevent gradient explosion, all normalized states are

clipped to [0, 2] and each gradient is capped at 40. Rewards are clipped to [-2, 2].

### 3 Calculation

We evaluated MA2C, IA2C, IQL-DNN and IQL-LR in SUMO-simulated traffic environments replicating two districts in the Bologna area (Andrea Costa and Pasubio) [15]. While these traffic networks are similar in the required number of agents, they differ significantly in their topology allowing evaluating how the latter influence the learning process. Every episode of the SUMO simulation consists of 3600 time steps. For a pre-determined interval of time, each time step a vehicle is inserted in the traffic network with a random Origin-Destination (OD) pair.

To ensure a fair evaluation of the algorithms, we have adopted identical settings for the experiment parameters except these parameters specific to each algorithm ([1]). The criterion used to evaluate the algorithms' performance is the queue at the intersections, which is linked to the DP reward by equation (2.2.1). Therefore, queues are estimated within SUMO for each crossing and then elaborated as rewards. In testing, the algorithms have been compared with a greedy approach (in the following referred as Greedy) which simply selects the traffic light phase associated with the largest green wave over all incoming lanes. For the pseudo stochastic experiments reported in the following sections, the seed is kept constant during training while different seeds are used in the 8 testing episodes <sup>8</sup>. For the fully stochastic experiment (reported in section 4), the seeds are kept constant only during each episode; when testing, seeds are changed for each of the 8 episodes,

---

<sup>8</sup>For all the tests and the totally random learning experiment, the seeds used are: 10400, 20200, 31000, 3101, 122, 42, 20200, 33333

Par.	Value	Description
$\alpha$	0.9	space weighting factor
$T_s$	3600 [s]	period of simulated traffic
$\Delta t$	5 [s]	interaction time between each agent and the traffic environment
$t_y$	2 [s]	yellow time
$N_v$	2000,3600 [veh]	total number of vehicles
$\gamma$	0.99	discount factor, controlling how much expected future reward is weighted
$\eta_\theta$	$5 \exp(-4)$	coefficient for $\nabla \mathcal{L}(\theta_i)$ used for gradient descent optimization
$\eta_\psi$	$2.5 \exp(-4)$	coefficient for $\nabla \mathcal{L}(\psi_i)$
$ B $	40	size of the batch buffer
$\beta$	0.01	parameter to balance the entropy loss of policy $\pi_{\theta_i}$ to encourage early-stage exploration

Table 1: IA2C and MA2C Settings

like in the pseudo-stochastic case.

The DP is finally instantiated with the settings listed in Table 1.

The size of the batch indirectly sets up the  $n$  parameter of the  $n$ -step return appearing in equation (5), (6), (7) and (8) and has been chosen balancing the complementing characteristics of TD and Monte-Carlo methods [12]. With a forward step limit at 1000800 and the settings reported in Table 1 for  $T_s$ ,  $\Delta t$  and  $|B|$ , a complete learning process results in 278 episodes (i.e. 5004 learning steps).

### 3.1 Algorithms

Our tests don't rely on a structured configuration of the vehicles in motion<sup>9</sup>. In fact, assuming a traffic macro-behavior in terms of general vehicle flows is beneficial when the flows effectively reflect the real traffic macro-behavior; but this is seldom the case in practice and such assumptions might instead cause overfitting [16] originating from spurious regularities. To avoid this issue, our stochastic approach assigns pseudo-random Origin Destinations (OD) pairs to each vehicle. This allows the learning process to achieve a more general optimum as the equilibrium among the agents doesn't depend on any specific assumption on the flows or boundary condition. Our experimentation consists of the following steps:

- Loading our traffic networks with a varying number of vehicles.
- Evaluating the training graphs of IQL-DNN and IQL-LR.
- Comparing the IA2C and MA2C learning curves
- Comparing MA2C with IA2C and Greedy
- Evaluating the behavior of the learning curves for IA2C and MA2C
- Evaluating the effects of the learned policies in terms of traffic volumes

### 3.2 Traffic Networks

Figure 5 (left) shows the Bologna - Andrea Costa neighborhood[15].

---

<sup>9</sup>In the main experiment (city of Monaco) performed in [1] vehicle flows on specific roads are predetermined; some randomness is allowed but affects only the position on the starting lane, while its path from its starting lane to its destination (eventually via specific points) is established

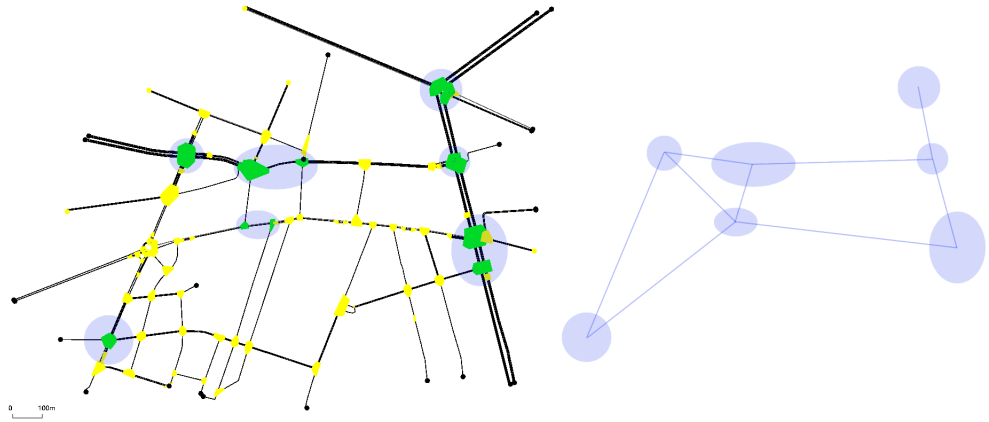


Figure 5: Andrea Costa

The round/elliptic (purple) shaded spots identify the signalized intersections (agents). The right side of the figure shows the way each agent is connected to the others. The set of all the agents connected to a single agent constitutes its neighborhood.

Figure 6 (left) shows the Bologna - Pasubio neighborhood [15]. As in the Andrea Costa case, the right hand side of the figure shows how the agents have been connected.

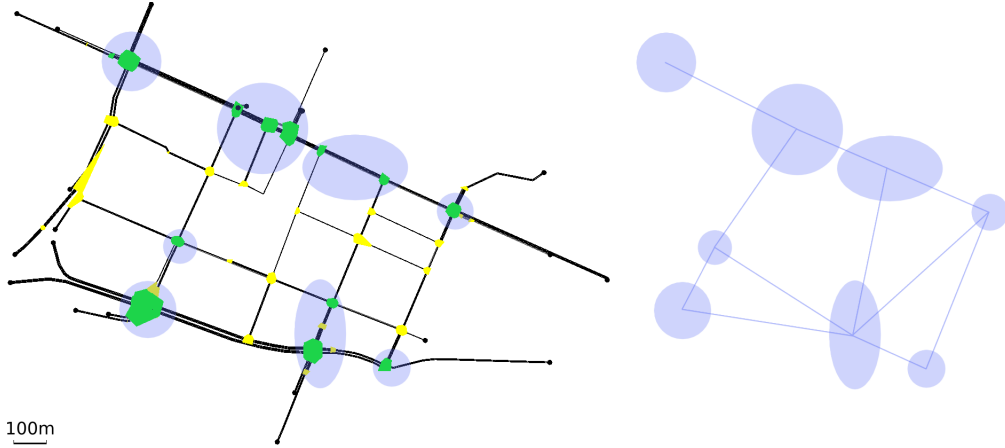


Figure 6: Pasubio

The vehicle insertion procedure consists of 3600 time steps and is divided into the following alternatives:

- 2000 vehicles in the first 2000 time steps, then no more vehicles for the remaining time steps
- 3600 vehicles in the 3600 time steps
- 4000 vehicles in the first 2000 time steps, then no more vehicles for the remaining time steps

### 3.3 IQL-DNN and IQL-LR

Coherently with the results reported in [1]<sup>10</sup> we found that the two algorithms IQL-DNN and IQL-LR perform rather poorly in our traffic networks even in the

---

<sup>10</sup>in [1] a good behavior of IQL-DNN and IQL-LR is reported only for basic (unrealistic) experiments; in fact in figure 9 and 10 in [1] they have been omitted due to their low performance with a real traffic network

simplest case (2000 vehicles). Figure 7 and 8 show the performance of the two algorithms in terms of the overall average queue<sup>11</sup>. The graphs show that the algorithms take a divergent trend and then stabilize around 500.000 interactions to a value significantly worse than the original setting <sup>12</sup>. In view of this results we excluded IQL-DNN and IQL-LR in further experimentation with real traffic networks, coherently with the line followed in [1].

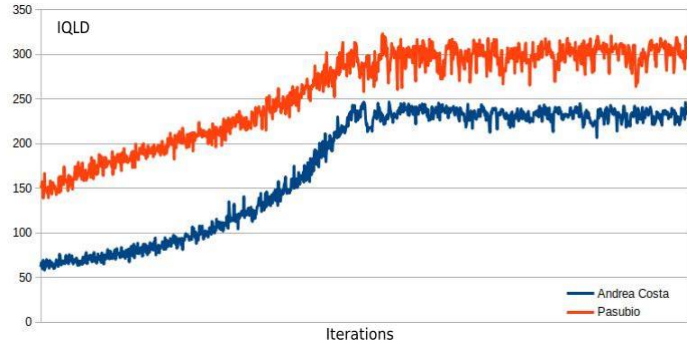


Figure 7: Average Queue while learning for IQL-DNN for the cases Andrea Costa and Pasubio.

---

<sup>11</sup>This quantity cumulates the contributions of all the signalized intersections and it is further averaged over the episode length; it will be referred simply as "average queue" in the next sections

<sup>12</sup>Similarly to all the other experiments reported, every learning process has been repeated ten times, with similar results

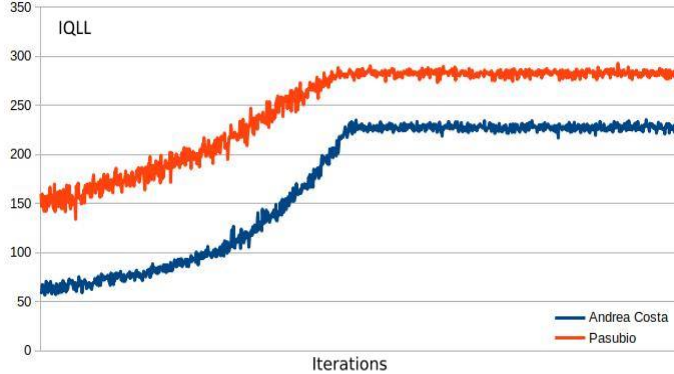


Figure 8: Average Queue while learning for IQL-LR for the cases Andrea Costa and Pasubio.

### 3.4 MA2C and IA2C performance on the A. Costa Traffic Network

Figure 9 and 10 show the minimization of the average queue on the traffic network loaded with 2000 and 3600 vehicles, respectively. While both the MA2C and IA2C learning processes achieve a similar minimum, the curves appear very different: while MA2C achieves a stable point from iteration  $\sim 100$  onward, IA2C is much less steady. Particularly in Figure 10 (load of 3600 vehicles), IA2C achieves its optimum (which, as shown in Figure 15 is the only success out of 10 learning runs) only in the very end of the process.

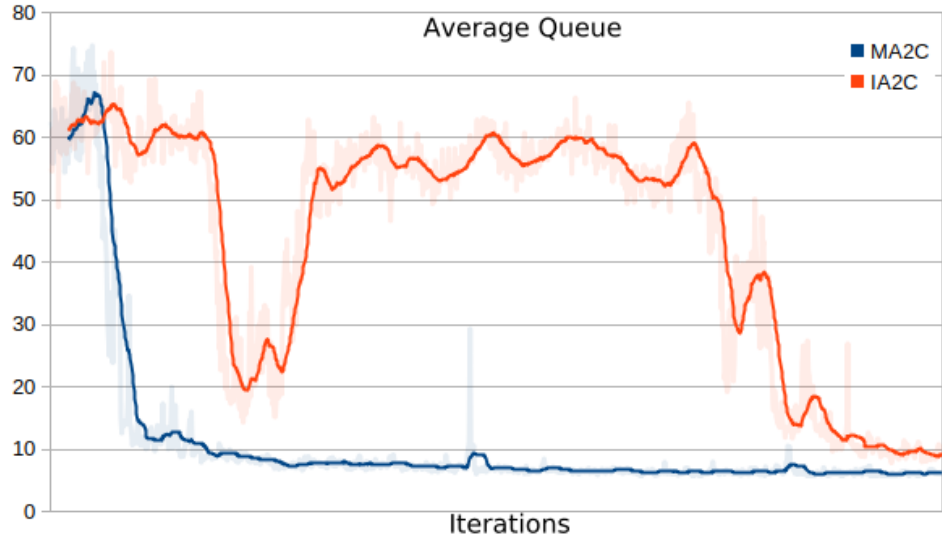


Figure 9: Andrea Costa, average queue, 2000 veh, IA2C and MA2C: training steps are shown on the horizontal axis.

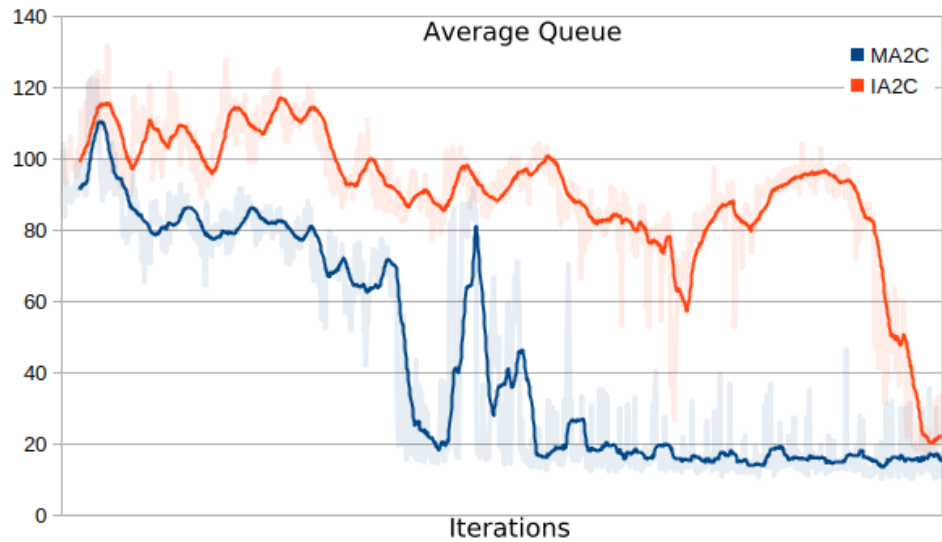


Figure 10: Andrea Costa, average queue, 3600 veh, IA2C and MA2C: training steps are shown on the horizontal axis.

Tables 2 and 3 show 8 tests performed by changing the random seeds and com-

Test	1	2	3	4	5	6	7	8	Ave	Std
<b>MA2C</b>	6.55	5.81	6.26	5.66	6.33	5.90	5.98	6.08	6.07	0.28
<b>IA2C</b>	8.38	8.43	8.36	8.15	7.8	8.09	8.7	8.75	8.33	0.30
<b>Greedy</b>	25.29	18.52	23.19	17.58	20.79	17.36	18.52	24.14	20.67	2.95

Table 2: Average Queue Test, Andrea Costa, 2000 veh.

Test	1	2	3	4	5	6	7	8	Ave	Std
<b>MA2C</b>	11.59	11.70	12.72	11.60	10.88	11.12	10.84	11.64	11.51	0.56
<b>IA2C</b>	18.89	18.88	20.72	19.55	17.56	19.75	18.06	19.25	19.08	0.92
<b>Greedy</b>	27.96	28.94	33.18	29.19	27.96	38.51	30.46	31.64	30.98	3.31

Table 3: Average Queue Test, A. Costa 3600 veh.

puting Average and Standard Deviation of the considered sample. MA2C appears better than IA2C in Table 2, and evidently outperforms Greedy.

The average queue measured is similar to the achieved minimum in the training process, showing that even though the system was trained with pseudo-random simulations, the final result doesn't appear to overfit on specific sets of origin-destination (O.D.) pairs. This is specially important because it certifies that the learning process doesn't focus in dynamics other than the ones occurring at the traffic lights vicinity. In fact, RL has a tendency to overfitting when the training dataset is a subset of all potential cases [16] and training with real data is a challenging task as transforming integrated traffic flow data into O.D. matrices requires mixed heuristic-deductive reasoning [17].

In the next sections this relevant finding will be confirmed by further experimentation.

Test	1	2	3	4	5	6	7	8	Ave	Std
<b>MA2C</b>	17.56	24.73	29.5	30.36	29.49	21.93	36.53	22.44	26.57	5.63
<b>IA2C</b>	61.22	79.24	70.99	73.06	70.06	101.67	57.67	29.47	67.92	19.16
<b>Greedy</b>	10.61	15.14	19.89	15.76	14.14	22.58	15.14	20.88	16.77	3.73

Table 4: Average Queue Test, Pasubio, 2000 veh.

Test	1	2	3	4	5	6	7	8	Ave	Std
<b>MA2C</b>	32.03	33.06	41.25	35.66	28.20	35.82	31.16	33.42	33.82	3.63
<b>Greedy:</b>	26.71	37.78	37.44	35.36	28.60	80.66	37.78	76.23	45.07	19.70

Table 5: Average Queue Test, Pasubio 3600 veh.

### 3.5 MA2C and IA2C on the Pasubio Traffic Network

Figure 11 shows the training graph for the case of 2000 vehicles circulating in the Pasubio traffic network. The figure shows that MA2C has been able to achieve an improvement while IA2C showed a much more wobbly behavior during training. As a result, when measuring performances with 8 different test seeds, the average queue measured are very different in the two cases (table 4 and 5). Notably, in table 4, MA2C exhibits a slightly worse behaviour when compared with the Greedy approach.

The case of 3600 vehicles showed more challenging for MA2C and IA2C (figure 12). While IA2C was unable to perform an optimization in the limit of 10 learning runs, MA2C was successful in 6 runs out of 10 (Figure 15). However when performing testing, MA2C was more effective than the Greedy policy, which showed a larger average and a much larger variance in the 8 tests.

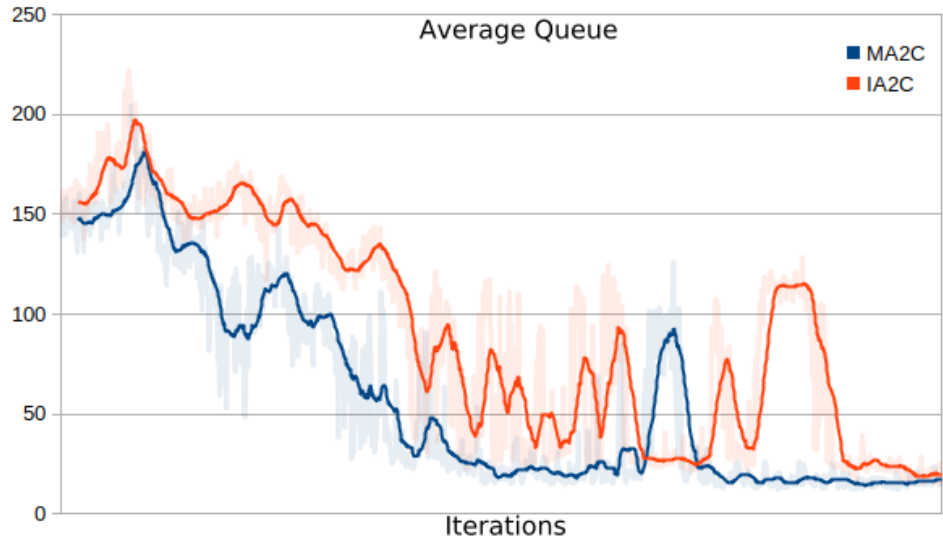


Figure 11: Pasubio IA2C and MA2C: average queue when loading the traffic network with 2000 vehicles in pseudo-random traffic conditions.

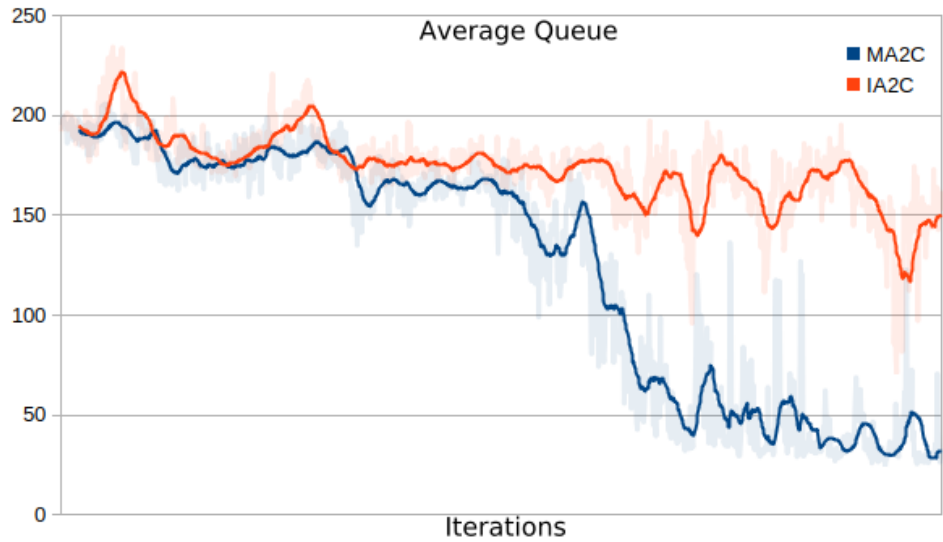


Figure 12: Pasubio, IA2C and MA2C: average queue when loading the traffic network with 3600 vehicles in pseudo-random traffic conditions.

### 3.6 Further Tests

To evaluate further the MA2C capabilities to manage a growing vehicle flow we experimented inserting two vehicles every time step for the time interval  $[0, 2000]$ , therefore inserting a total of 4000 vehicles in the traffic network. We repeated the experiment for the usual 10 training attempts both for the Andrea Costa and Pasubio traffic networks. In all our attempts MA2C showed a consistent behaviour by diverging in the initial training stage to start learning in the following steps, but it substantially shows unable to achieve a significant improvement in terms of the average queue of vehicles as shown in figure 13.

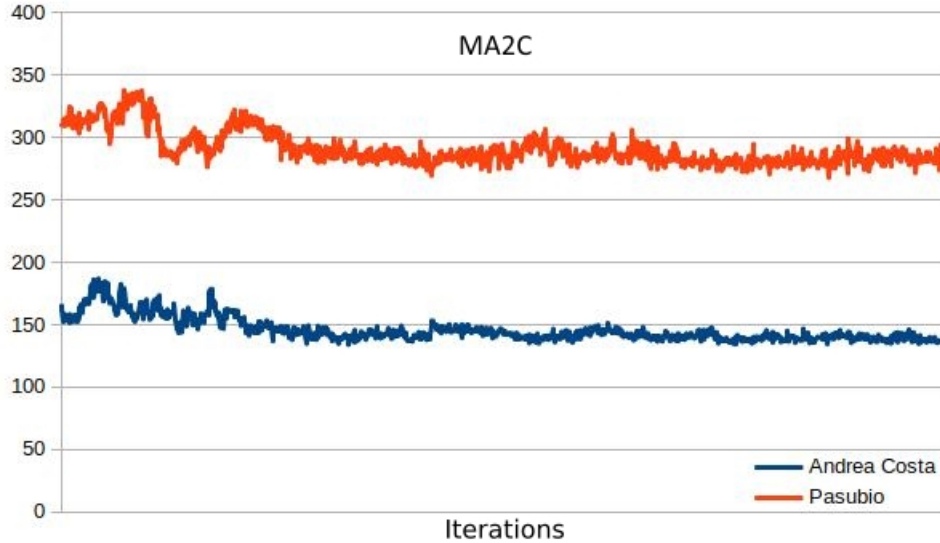


Figure 13: MA2C: average queue when loading the traffic network with 4000 vehicles in the time interval  $[0-2000]$ , in pseudo-random traffic conditions.

Though this behaviour highlights MA2C's limitations in dealing with high volumes of traffic, we will see in the next sections that MA2C still represents a better alternative of the other algorithms even in this case.

## 4 Evaluation of the learning process of MA2C and IA2C

Work on convergence of actor-critic decentralized MARL has been reported in [18], [16] and [19]. However, all these studies relies on underlying Markov Chains; furthermore [18] and [16] rely on linear function approximation, [16] refers fully decentralized agents and in [19] agents do not share information about their local policy: all these hypotheses do not hold for the presented algorithms. To the best of the authors' knowledge, a theory encompassing all the features of MA2C (Long Short-Term Memory Networks, restricted communication among neighboring agents, non-linearity of the function approximation, etc) is still missing. However, some heuristic analysis is possible by inspecting the Average Queue curve during learning. A tendency to diverge from an asymptotic behaviour, the presence of wobbles or spikes shows that the agents didn't find a steady balance among them: even when a solution able to smooth the overall vehicle flow is found, queues at each signalized intersection can concurrently shrink and grow up to a limit.

### 4.1 Evaluation of the learning process

When ANNs are coupled with Reinforcement Learning, a challenging task arises from pursuing a changing target during the learning process. In the multi-agent case, targets are even more elusive: an agent, e.g. agent  $i$ , converges smoothly towards an optimal policy as long as  $\theta_{-i}$  stay constant, but this is not the case in a collective learning process where other agents' changing policies  $\pi_{\theta_{-i}}$  affect their behaviour, which, in turn, affects (from the decentralized view point) the expected

return of agent  $i$ . Eventually, this sequence of causal relationships might make inconsistent the learning process. This issue can happen even if agent  $i$  found an ideal policy: changes of  $\pi_{\theta_{-i}}$  might cause the agent  $i$  to slip from its optimum. An ideal situation present itself when all the agents find their optima (approximately) at the same time. As an example of this problem Figure 14 shows the behaviour of the seven agents in the Andrea Costa case, when loaded with 2000 vehicles, meaning that for the first 2000 time steps of the overall 3600 time steps of the episode, one vehicle is pseudo-randomly inserted on the traffic network at each time step while for the remaining 1600 time steps (once the number of inserted vehicles reaches 2000) no "new" vehicle is inserted. The top graphs show the behaviour in time of the Actor's loss for agents  $a_0, \dots, a_6$  during the learning process. The bottom picture represents the reward graph, showing as the averaged cumulative queues evolve in time. The left hand side (red) shaded region highlights the inconsistency issue: at the beginning of the shaded region agent  $a_1$  is slightly unstable (while the other agents appear to be close to a relative balance) and eventually drags away the other agents from their converging path. In the (green) shaded region on the right hand side, instead, all the agents appear to move coherently towards a common relative minimum; this is especially evident observing agent 0, 1 and 4 while the other agents cost shows that they are close to a common balance.

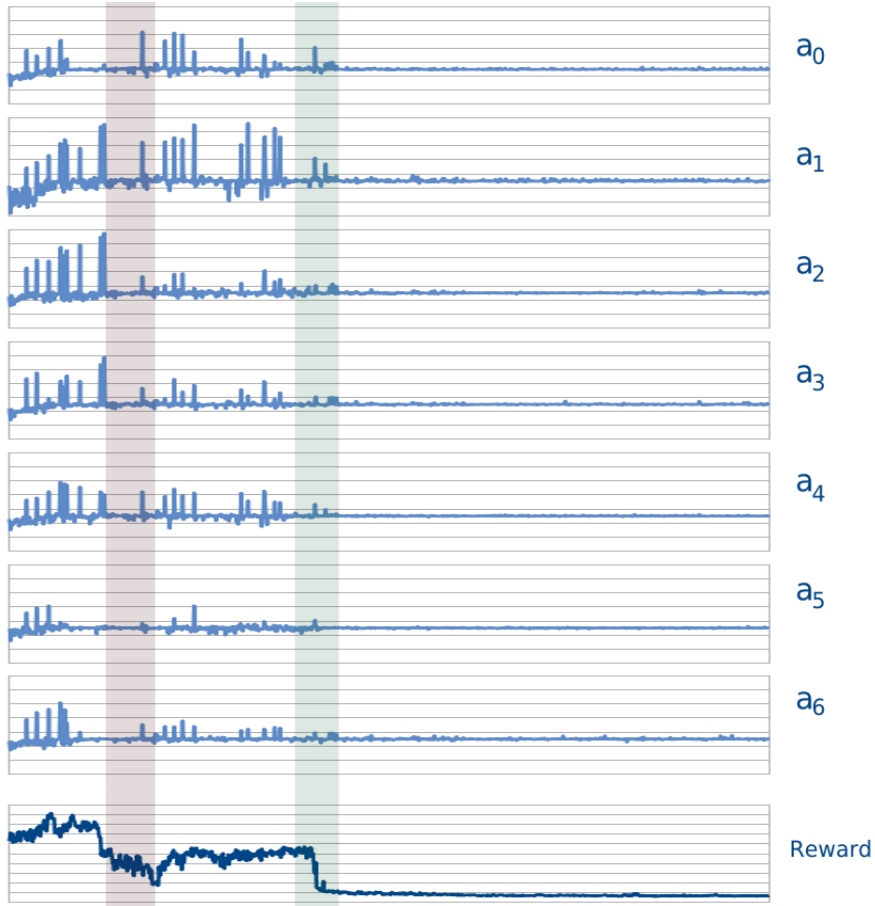


Figure 14: A. Costa learning graphs showing the evolution in time of seven agents' loss ( $a_0, \dots, a_6$ ) and their accrued Reward when the traffic network is loaded with 2000 vehicles. The left hand side (red) shaded region highlights the inconsistency issue: at the beginning of the shaded region agent  $a_1$  is slightly unstable (while the other agents appear to be close to a relative balance) and eventually drags away the other agents from their converging path. In the (green) shaded region on the right hand side, instead, all the agents appear to move coherently towards a common relative minimum.

To limit the occurrence of such inconsistencies it is beneficial to maintain the learning process as smooth as possible; this is achieved by keeping small

$D_{KL}(\pi_{\theta-}, \pi_{\theta})^{13}$  by updating the target of the optimization process after each learning step.

The overall consistency of the algorithms during training can be evaluated by observing that the properties of the environment change significantly depending on quantitative factors. For this reason, we compared the results obtained with IA2C and MA2C in three experimental settings with varying number of vehicles introduced in the traffic networks: Figure 15 shows our results when running 10 learning experiments for the cases with 1000, 2000 and 3600 vehicles in both the A. Costa and Pasubio networks.

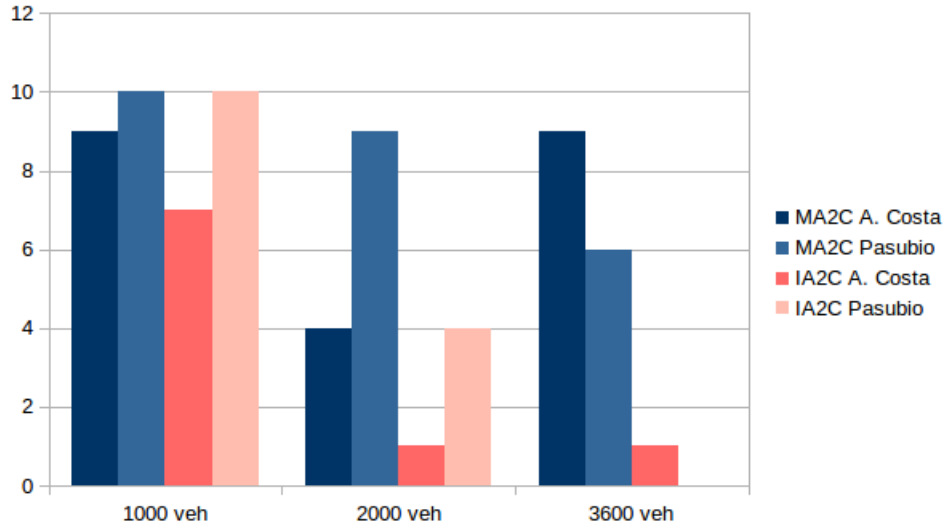


Figure 15: Learning stability while training with the Andrea Costa Traffic Network, loaded with 2000 veh.

As evident in Figure 15, MA2C shows more stable than IA2C. Moreover, the learning processes tend to become more inconsistent when the vehicle load increases, with the notable exception of the A. Costa case loaded with 2000 veh,

<sup>13</sup> $D_{KL}$  is the Kullback–Leibler divergence

which shows much more problematic than the case with 3600 veh. It is interesting to observe that, while this case shows more unsteady than the 3600 case, the graph of the A. Costa case loaded with 2000 vehicles displays a much less wavy behaviour once convergence is achieved, as highlighted in the Figure 16 (shaded region).

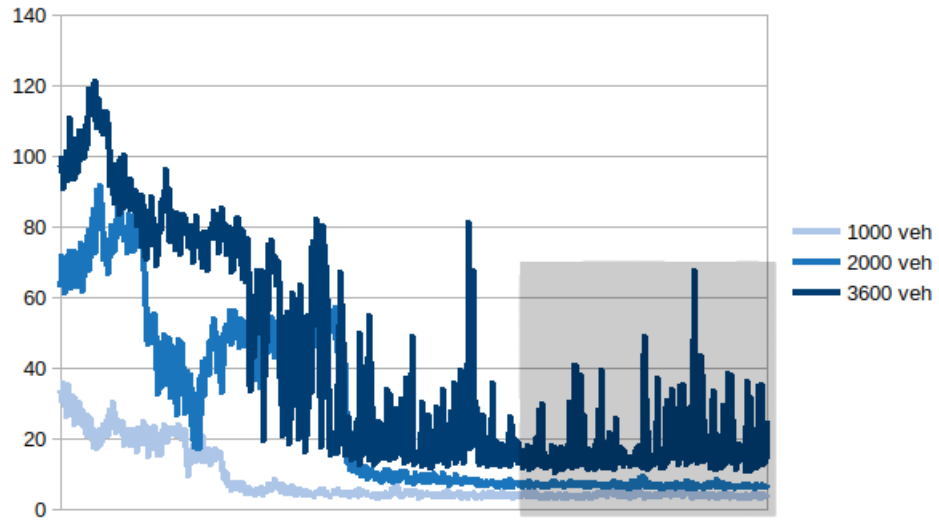


Figure 16: Loss behaviour in the A. Costa case (1000, 2000 and 3600 veh). When loaded with 1000 or 2000 vehicles, the achieved convergence stays stable while, when loaded with 3600 veh, the agents "keep struggling" even after reaching a balance among them.

Figure 16 shows that, when loaded with 1000 or 2000 vehicles, the achieved convergence stays stable while, when loaded with 3600 veh, the agents "keep struggling" even after reaching a balance among them, due to the excessive amount of vehicles circling on the traffic network.

## 4.2 Random flow learning

To test the attitude of the considered algorithms towards focusing on the signalized intersection dynamics, we attempted training using totally random vehicle flows. This test differs from the previous ones as the random process seeds change at every simulation instead of staying constant through the whole learning process. When injecting in the traffic networks one vehicle per time step, we found the no algorithm among the ones considered was able to achieve positive results with the notable exception of the traffic network in Figure 6. In this setting only MA2C was able to optimize a policy within our 10 attempts (Figure 17).

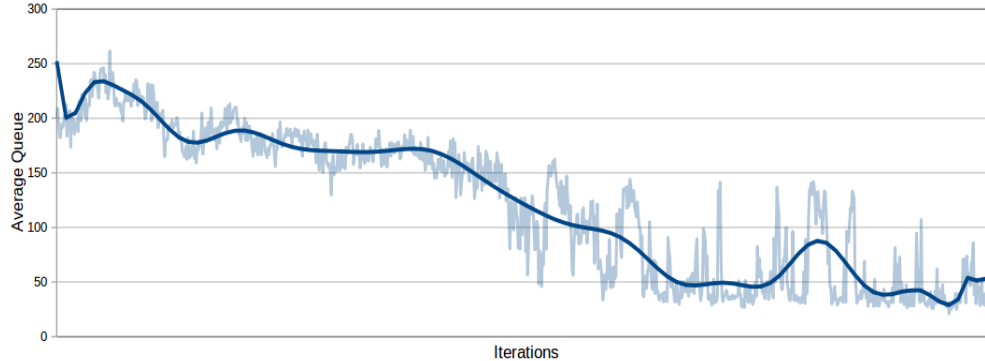


Figure 17: Pasubio, MA2C: average queue when loading the traffic network with 3600 vehicles in random traffic conditions.

However, when testing by changing the random seeds we found that no better performance was achieved with respect to the pseudo-random case.

Table 6 shows that the MA2C performance with random traffic is slightly worse than in the pseudo-random case.

This experiment confirms that pseudo-random training is a well-balanced approach: its performance when changing the seeds (and therefore changing the

Test	1	2	3	4	5	6	7	8	Ave	Std
<b>P. Random</b>	32.03	33.06	41.25	35.66	28.20	35.82	31.16	33.42	33.82	3.63
<b>Random</b>	31.54	35.45	59.39	33.29	28.73	49.50	34.56	40.45	39.11	9.71

Table 6: MA2C, Average Queue Test, Pasubio, 3600 veh., Pseudo Random and Totally Random Traffic

vehicle distribution in terms of origin-destination pairs) shows that it is capable to avoid overfitting to spurious traffic circumstances and, at the same time, it presents to the algorithms’ optimization procedure a more manageable learning problem than the one posed by total-random training.

### 4.3 Generalization Analysis

In this section we present another strategy to evaluate MA2C attitude towards overfitting. So far we evaluated a certain solution only with its respective test cases; for instance we tested a policy learned with 2000 vehicles with the same number of vehicles (though in different vehicle distributions). In this section we cross-test the result of the learning step with varying vehicle loads. For instance, we test MA2C to see how well the policy learned with 2000 vehicles performs with 3600 vehicles. These experiments have relevance as they contribute to help assessing the quality of pseudo-random training by allowing evaluating how much our agents are able to focus on the vehicle dynamics at their surroundings resisting overfitting to other spurious features such as the vehicle load and distribution in time and space. The tables in the next sections report the results of our experiments.

### 4.3.1 Training MA2C with 2000 vehicles

Table 7 shows the results of MA2C with respect of Greedy. On average, In the six experiments reported, MA2C outperforms the greedy approach in five of them, with the notable exception of via Pasubio when testing with 2000 vehicles. It is interesting that, though trained with 2000 vehicles, MA2C keeps performing well when dealing with 3600 vehicles indicating that the learned policy does focus on the dynamics of the vehicle in the agents' proximity. Finally, while seemly intractable for 4000 vehicles in 2000 time steps, when MA2C failed to learn a policy, the chaotic traffic related to this case can be alleviated by using the policy learned with 2000 vehicles, which performs slightly but evidently better than Greedy.

A. Costa									
Testing: 2000 veh.								<b>Ave</b>	<b>Std</b>
<b>MA2C</b>	6.55	5.81	6.26	5.66	6.33	5.90	5.98	6.08	6.07
<b>Greedy</b>	25.29	18.52	23.19	17.58	20.79	17.36	18.52	24.14	20.67
Testing: 3600 veh.								<b>Ave</b>	<b>Std</b>
<b>MA2C</b>	9.20	8.9	28.54	20.69	9.16	8.73	8.86	9.09	12.90
<b>Greedy</b>	27.96	28.94	33.18	29.19	27.96	38.51	30.46	31.64	30.98
Testing: 4000 veh.								<b>Ave</b>	<b>Std</b>
<b>MA2C</b>	133.3	141.6	143.6	140.2	131.9	144.0	140.3	138.3	139.1
<b>Greedy</b>	163.2	161.15	168.3	163.1	154.9	166.6	161.1	162.5	162.6
Pasubio									
Testing: 2000 veh.								<b>Ave</b>	<b>Std</b>
<b>MA2C</b>	17.56	24.73	29.5	30.36	29.49	21.93	36.53	22.44	26.57
<b>Greedy</b>	10.61	15.14	19.89	15.76	14.14	22.58	15.14	20.88	16.77
Testing: 3600 veh.								<b>Ave</b>	<b>Std</b>
<b>MA2C</b>	32.03	33.06	41.25	35.66	28.20	35.82	31.16	33.42	33.82
<b>Greedy</b>	26.71	37.78	37.44	35.36	28.60	80.66	37.78	76.23	45.07
Testing: 4000 veh.								<b>Ave</b>	<b>Std</b>
<b>MA2C</b>	255.9	240.7	241.6	267.4	261.6	255.4	248.8	250.7	252.7
<b>Greedy</b>	257.3	251.3	259.4	273.0	275.0	263.2	251.4	262.4	261.6

Table 7: Average Queue Cross Test, MA2C trained with 2000 vehicles

### 4.3.2 Training MA2C with 3600 vehicles

Table 8 shows our results when training MA2C with 3600 vehicles. In all the experiments MA2C showed better performances than Greedy. It is noticeable that in the via Pasubio case, MA2C trained with 3600 performs better than MA2C trained with 2000 vehicles, even when tested with 2000 vehicles.

A. Costa									
Testing: 2000 veh.								<b>Ave</b>	<b>Std</b>
<b>MA2C</b>	7.78	7.22	7.05	7.92	7.05	7.32	7.20	7.16	7.33
<b>Greedy</b>	25.29	18.52	23.19	17.58	20.79	17.36	18.52	24.14	20.67
Testing: 3600 veh.								<b>Ave</b>	<b>Std</b>
<b>MA2C</b>	10.84	11.59	17.59	11.70	12.90	12.72	11.60	10.88	12.48
<b>Greedy</b>	27.96	28.94	33.18	29.19	27.96	38.51	30.46	31.64	30.98
Testing: 4000 veh.								<b>Ave</b>	<b>Std</b>
<b>MA2C</b>	132.9	142.4	139.3	144.8	137.3	144.7	140.5	140.0	140.2
<b>Greedy</b>	163.2	161.15	168.3	163.1	154.9	166.6	161.1	162.5	162.6
Pasubio									
Testing: 2000 veh.								<b>Ave</b>	<b>Std</b>
<b>MA2C</b>	14.82	17.00	18.44	18.09	21.20	22.57	20.60	20.84	19.20
<b>Greedy</b>	10.61	15.14	19.89	15.76	14.14	22.58	15.14	20.88	16.77
Testing: 3600 veh.								<b>Ave</b>	<b>Std</b>
<b>MA2C</b>	23.10	28.91	22.51	23.66	22.09	38.23	25.16	33.42	30.6
<b>Greedy</b>	26.71	37.78	37.44	35.36	28.60	80.66	37.78	76.23	45.07
Testing: 4000 veh.								<b>Ave</b>	<b>Std</b>
<b>MA2C</b>	241.5	248.8	244.1	272.9	259.2	248.6	250.9	253.5	252.5
<b>Greedy</b>	257.3	251.3	259.4	273.0	275.0	263.2	251.4	262.4	261.6

Table 8: Average Queue Cross Test, MA2C trained with 3600 vehicles

## 5 Results

Overall, our experiments show that MA2C outperforms both IA2C and the Greedy approach by exhibiting a more robust behaviour when aiming to reduce the ve-

hicle queues at signalized intersections. In this section we evaluate how MA2C performance translates in terms of general traffic flows.

To this end we focus to the A. Costa experiment when loaded with 2000 vehicles. As described in the above sections, our typical traffic simulation spans over 3600 time steps, with an interaction time of each vehicle with its environment of 5 s (table 1):

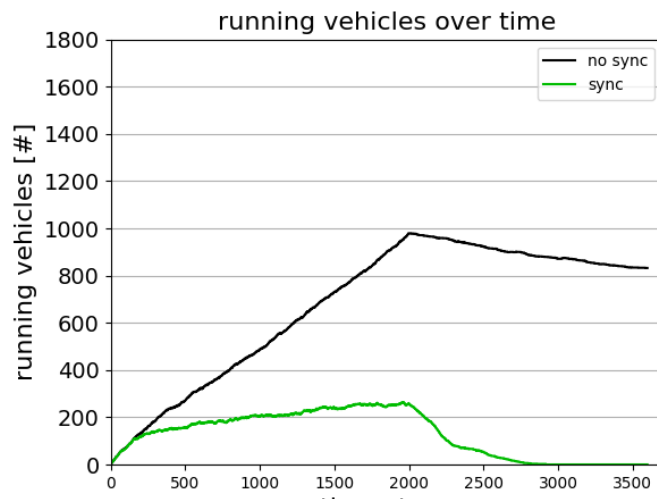
- In the first part of the simulation (time steps  $[0, 2000]$ ) a vehicle is pseudo-randomly inserted on the map for each time step and follows a pseudo-random path.
- In the second part of the simulation (time steps  $[2000, 3600]$ ) no vehicle is inserted. Eventually, all the vehicles circulating on the map leave through one of the exit lanes or end their journey by reaching their destination.

Figure 18 shows the number of running vehicles in the time span  $[0, 3600]$  for the cases Andrea Costa and Pasubio:

The curve referring to the beginning of the training (No Sync case) - when a synchronisation among the agents is yet to be achieved - shows that due to heavy queuing at the traffic lights, several vehicles stay on the road after time step 2000. In the graph, the curve keeps rising while vehicles are injected and tends to slowly decrease afterwards. When synchronization occurs (Sync case), the amount of vehicles running fades quickly towards zero after time step 2000.



(a) Andrea Costa



(b) Pasubio

Figure 18: Running vehicles over time

## 6 Discussion

The development of multi-agent reinforcement learning methods for real-life problems constitutes a promising research area, which, however, is still in its initial phase [20], due to the complications arising when seeking a balance in a cooperative-competitive stochastic game.

In this paper we analyzed four multi-agent reinforcement learning algorithms, namely IQL-DNN, IQL-LR, IA2C and MA2C. Moreover, we reformulated the theory of IA2C, ([1]) and MA2C, ([1], [2]) adopting the formalism of non-Markov Decision Process. Finally we evaluated the algorithms in traffic networks in two areas of Bologna (Italy) replicated in SUMO, a software tool for ATSC problems. Our results indicate that MA2C, which operates on the basis of reward calculated locally and exploits a form of communication between nearby agents, achieves good performance in the majority of cases and outperforms the alternative methods considered. The analysis of the learning process and the comparison of the results obtained by varying the number of vehicles also indicates that MA2C is sufficiently effective although it showed unable to converge when the number of circulating vehicles raised above a limit. The analysis of the results obtained by training the system with pseudo-random vehicles and post-evaluating it with total random traffic demonstrates that this technique resists overfitting. This finding constitutes a relevant step to tackle real-world traffic problems with MARL algorithms. Concerning future research, our experiments show that finding a balance among the agents' actions is conditioned by the number, variety and inter-connections of the agents and by the traffic volume. To simplify the task it appears adequate to split traffic networks graphs in subgraphs. This strategy can be more efficiently

performed using less densely intra-related traffic networks as benchmark, such as areas in the outskirts of cities, which are more suitable to be split in sub-areas as agents (signalized intersections) tend to cluster in small groups. Remarkably, loading the networks with pseudo-random vehicle flows, turns beneficial to such a design, as it avoids the need of connecting traffic flows among adjacent areas.

## 7 Conclusions

In this work we originally formulate the theory of Independent Advantage Actor Critic (IA2C, [1]) and Multi-Agent Advantage Actor Critic (MA2C, [1], [2]) adopting the formalism of non-Markov Decision Process. Our formulation provides a comprehensive view of the algorithms' inner machinery, casting insights for future developments. In addition, we evaluate MA2C in multiple adaptive traffic signal control (ATSC) problems and compare it with other algorithms. Our tests show that training with pseudo-random traffic flows yields robust policies and resist overfitting, establishing itself as an effective technique to train Multi-Agent Reinforcement learning algorithms for ATSC.

Generally, our experiments show that MA2C outperforms the other options, presenting itself as a promising approach for further research.

## CRediT

**Paolo Fazzini:** Project Administration, Conceptualization, Methodology, Formal Analysis, Investigation, Software, Validation, Visualization, Writing- Original draft preparation. **Isaac Wheeler:** Writing- Reviewing and Editing. **Francesco**

**Petracchini:** Supervision, Resources.

## Acknowledgments

We thank Dr. Stefano Nolfi for his insightful advising. This research did not receive any specific grant from funding agencies in the public, commercial, or not-for-profit sectors. The authors have no competing interests to declare.

Color should not be used for any figures in print.

## References

- (1) Chu, T.; Wang, J.; Codecà, L.; Li, Z. Multi-Agent Deep Reinforcement Learning for Large-scale Traffic Signal Control, 2019.
- (2) Chu, T.; Chinchali, S.; Katti, S. Multi-agent Reinforcement Learning for Networked System Control, 2020.
- (3) Lopez, P. A.; Wiessner, E.; Behrisch, M.; Bieker-Walz, L.; Erdmann, J.; Flotterod, Y.-P.; Hilbrich, R.; Lucken, L.; Rummel, J.; Wagner, P. In *2018 21st International Conference on Intelligent Transportation Systems (ITSC)*, 2018 21st International Conference on Intelligent Transportation Systems (ITSC), IEEE: Maui, HI, 2018, pp 2575–2582.
- (4) Hunt, P.; Robertson, D.; Bretherton, R. D.; Royle, M. *Traffic engineering and control* **1982**, *23*.
- (5) Luk, J. In 1983.
- (6) Gokulan, B. P.; Srinivasan, D. *IEEE Transactions on Intelligent Transportation Systems* **2010**, *11*, 714–727.
- (7) Chiu, S.; Chand, S. In *Proceedings. The First IEEE Regional Conference on Aerospace Control Systems*, 1993, pp 122–126.
- (8) Teodorović, D. *Transportation Research Part C: Emerging Technologies* **2008**, *16*, 651–667.
- (9) Lee, J.; Abdulhai, B.; Shalaby, A.; Chung, E.-H. *Journal of Intelligent Transportation Systems* **2005**, *9*, 111–122.

(10) Wierstra, D.; Förster, A.; Peters, J.; Schmidhuber, J. In *ICANN'07*, Springer: Berlin, Germany, 2007, pp 697–706.

(11) Williams, R. J. *Machine Learning* **1992**, *8*, 229–256.

(12) Sutton, R. S.; Barto, A. G., *Reinforcement learning: an introduction*; Adaptive computation and machine learning; MIT Press: Cambridge, Mass, 1998; 322 pp.

(13) Barto, A. G.; Sutton, R. S.; Anderson, C. W. *IEEE Transactions on Systems, Man, and Cybernetics* **1983**, *SMC-13*, 834–846.

(14) Mnih, V.; Badia, A. P.; Mirza, M.; Graves, A.; Lillicrap, T. P.; Harley, T.; Silver, D.; Kavukcuoglu, K. *CoRR* **2016**, *abs/1602.01783*.

(15) Bieker, L.; Krajzewicz, D.; Morra, A. P.; Michelacci, C.; Cartolano, F. *Lecture Notes in Control and Information Sciences* **2015**, *13*, 47–60.

(16) Zhang, C.; Vinyals, O.; Munos, R.; Bengio, S. A Study on Overfitting in Deep Reinforcement Learning, 2018.

(17) Bera, S.; Rao, K. V. *European Transport Trasporti Europei* **2011**, *49*, 2–23.

(18) Grosnit, A.; Cai, D.; Wynter, L. Decentralized Deterministic Multi-Agent Reinforcement Learning, 2021.

(19) Zhang, Y.; Zavlanos, M. M. *CoRR* **2019**, *abs/1903.09255*.

(20) Irpan, A. Deep Reinforcement Learning Doesn't Work Yet, <https://www.alexirpan.com/2018/02/14/rl-hard.html>, 2018.